

This is a preprint of an article published in Journal of Experimental Botany. The final authenticated version is available online at: <https://doi.org/10.1093/jxb/erab404>

Three-dimensional quantitative analysis of the Arabidopsis quiescent center

Ran Lu^{1,2}, Balkan Canher^{1,2}, Anchal Bisht^{1,2}, Jefri Heyman^{1,2} and Lieven De Veylder^{1,2,*}

¹ Department of Plant Biotechnology and Bioinformatics, Ghent University, 9052 Gent, Belgium

² Center for Plant Systems Biology, VIB, 9052 Gent, Belgium

* Correspondence: lieven.deveylder@psb.vib-ugent.be

Corresponding author:

Lieven De Veylder

VIB Center for Plant Systems Biology

Ghent University, Department of Plant Biotechnology and Bioinformatics

Technologiepark 71

B-9052 Gent (Belgium)

Tel.: +32 9 3313961; Fax: +32 9 3313809; E-mail: lieven.deveylder@psb.vib-ugent.be

Abstract

Quiescent center (QC) cells represent an integral part of the root stem cell niche. They typically display a low division frequency that has been reported to be controlled by hormone signaling and different regulators, including the ERF115 transcription factor and D-type cyclins. Here, we applied a three-dimensional (3D) imaging pipeline to visualize the Arabidopsis QC cell number, volume and division patterns, including the visualization of anticlinal divisions that cannot be deduced from longitudinal 2D imaging. We found that five-day-old seedlings possess on average eight QC cells which are organized in a monolayered disk. In a period of seven days, half of the QC cells undergo anticlinal division in a largely invariant space. Ectopic expression of *ERF115* and *CYCD1;1* promote both anticlinal and periclinal QC cell divisions, the latter resulting in a dual-layered QC zone holding up to twofold more QC cells, compared to the wild type. Contrary, application of cytokinin or ethylene results in an increase in the number of periclinal but a decrease in anticlinal QC divisions, suggesting that they control the orientation of QC cell division. Our data illustrate the power of 3D visualization in revealing unexpected QC characteristics.

Running Title

Three-dimensional QC visualization

Highlight

Three-dimensional imaging allowed to visualize both anticlinal and periclinal Arabidopsis QC cell divisions, highlighting unexpected proliferation patterns in response to transgenes and hormone treatments.

Keywords

Arabidopsis, Cell division, *CYCD1;1*, Cytokinin, ERF115, Ethylene, MorphoGraphX, Quiescent center, Root meristem

Abbreviations

ACC: 1-amino-1-cyclopropane carboxylic acid; BA: 6-benzylaminopurine; CEI: cortex/endodermal initial; ERF115: ethylene response factor 115; WOX5: WUSCHEL-RELATED HOMEODOMAIN5; QC: quiescent center; SRDX: SUPERMAN REPRESSOR DOMAIN

Introduction

Root growth and development largely depend on a group of stem cells within the root apical meristem. Within *Arabidopsis thaliana*, these stem cells consist of quiescent center (QC) cells being surrounded by a single tier of initial cells that give rise to the different root cell types, including the lateral root cap, epidermis, cortex, endodermis, vasculature and columella (Dolan *et al.*, 1993). Here, the cortical and endodermal cell layers are derived from the same cortex/endodermal initial (CEI) cells. Likewise, the epidermis and lateral root cap tissues originate from a common stem cell. Since the concept of QC was proposed (Clowes, 1954), it has aroused great interest. As implicated by their name, the QC cells are characterized by a low division rate and are located at the center of the root stem cell niche. The QC cells inhibit the differentiation of the adjacent stem cells in a short-range manner (van den Berg *et al.*, 1997), whereas their periodical cell division probably enables the replacement of surrounding initial cells when required (Kidner *et al.*, 2000). Indeed, QC cell division activity is typically called upon under stress conditions, where the resulting daughter cells replace potentially damaged stem cells (Cruz-Ramírez *et al.*, 2013; Efroni *et al.*, 2016; Heyman *et al.*, 2013; Sena *et al.*, 2009). These unique properties bring to light the particular role played by the QC in maintaining the meristem structure and function.

It is well recognized that the QC cells are characterized by a low proliferation rate, compared to their surrounding initial cells, as suggested by ³H-thymidine or bromodeoxyuridine labeling experiments (Dolan *et al.*, 1993; Fujie *et al.*, 1993). According to a 5-ethynyl-2'-deoxyuridine (EdU) pulse-chase experiment, the time for QC cells to enter the S-phase can vary from three up to seven days (Cruz-Ramírez *et al.*, 2013). Consequently, the division frequency of QC cells was proposed to be even less than half that of the surrounding stem cells. Using a low laser power and a high scan rate to avoid photobleaching and phototoxicity, the longest reported imaging window under dark conditions for capturing *Arabidopsis* root meristem cell divisions is one week. During this 168-h time span, only a single QC cell was observed to divide, suggesting that the mitotic frequency of QC cells can be as low as one division in seven days (Rahni and Birnbaum, 2019). Consequently, to date, precisely describing the developmentally regulated QC cell division patterns remains challenging.

Several regulators of QC cell identity and division have been described. The PLETHORA and SCARECROW/SHORTROOT transcription factors are required in parallel for QC specification and root stem cell maintenance (Aida *et al.*, 2004; Sabatini *et al.*, 2003). A transcription factor gene encoding a core component of QC identity is *WUSCHEL-RELATED HOMEBOX5* (*WOX5*), which is specifically expressed in the QC (Haecker *et al.*, 2004; Sarkar *et al.*, 2007). *WOX5* represses, in a non-cell autonomous manner, the differentiation of the neighboring

columella stem cells (Pi *et al.*, 2015) and contributes in sustaining the quiescence of QC cells during embryogenesis by directly inhibiting the expression of the D-type cyclin-encoding gene *CYCD3;3* (Forzani *et al.*, 2014). The increased QC cell division rate observed *wox5* mutants can be suppressed by mutants in *CYCD1;1* or *CYCD3;3*, whereas their ectopic expression driven from the *WOX5* promoter is sufficient to induce QC cell division (Forzani *et al.*, 2014). The ethylene response factor 115 (ERF115) transcription factor represents another important rate-limiting factor in the QC cell division that is antagonistically regulated by proteolytic destruction through ubiquitination by the anaphase-promoting complex/cyclosome and transcriptional activation by brassinosteroid and jasmonic acid signaling (Heyman *et al.*, 2013; Zhou *et al.*, 2019). Next to controlling QC cell division, *ERF115* expression is also activated in cells localized immediately adjacent to dying meristematic cell, such as induced by DNA damaging agents, laser ablation or mechanical wounding (Heyman *et al.*, 2016; Hoermayer *et al.*, 2020; Matosevich *et al.*, 2020). Together with a wound-induced local accumulation of auxin, ERF115 induces cell divisions, generating new cells that eventually will replace the damaged ones (Canher *et al.*, 2020). Overexpressing the dominant negative *ERF115* allele fused with the *SUPERMAN REPRESSOR DOMAIN (SRDX)* dramatically reduces the frequency of these cell divisions, resulting in the inability to replace lost cells, followed by meristematic collapse (Canher *et al.*, 2020; Heyman *et al.*, 2016; Heyman *et al.*, 2013).

Next to genetic players, plant hormones play a key role in maintaining QC homeostasis. The directional flow of auxin in the root tip generates an auxin gradient, in which the maximum specifies the location of the QC (Grieneisen *et al.*, 2007). QC cell division is promoted by ethylene, with the resulting daughter cells maintaining QC identity and function, rather than adopting a stem cell-like fate (Ortega-Martínez *et al.*, 2007). Likewise, increasing cytokinin levels through genetic mutation or by exogenous application induces QC cell division by the direct downregulation of *Auxin transporter-like protein 2*, encoding an auxin influx carrier, and subsequent decrease in auxin levels (Zhang *et al.*, 2013). In contrast to ethylene, cytokinin-induced QC cell divisions are accompanied by a partial loss of QC identity, as observed by a decrease in *WOX5* expression (Zhang *et al.*, 2013). In addition to ethylene and cytokinin, other phytohormones including brassinosteroids, jasmonic acid and salicylic acid have been demonstrated to activate QC cell division (Chen *et al.*, 2011; González-García *et al.*, 2011; Lozano-Elena *et al.*, 2018; Vilarrasa-Blasi *et al.*, 2014; Zhou *et al.*, 2019), whereas abscisic acid has been shown to inhibit QC division (Zhang *et al.*, 2010).

Even though research focusing on the QC has been going on for decades, there is still no clear consensus on the exact *Arabidopsis* QC cell number and their division patterns. Originally, four QC cells were observed and described for the heart stage embryo, transverse sections of dry seeds and three-day-old seedlings (Dolan *et al.*, 1993). Later, 4-to-8 QC cells were observed

in transversal sections of mature embryos and less than one-week-old roots (Baum *et al.*, 2002; Ugartechea-Chirino *et al.*, 2010). These quantitative observations on QC cells were based on spatial location rather than use of any genetic marker, and therefore didn't attract widespread attention. As a consequence, a vast majority of researchers still agree on the consensus of the number of QC cells being four (Drisch and Stahl, 2015; Ortega-Martínez *et al.*, 2007; Rovere *et al.*, 2016; Zhang *et al.*, 2010) and only a few reported the number of QC cells to reach up to eight (Nawy *et al.*, 2005; Zhang *et al.*, 2013). This discrepancy might originate from the fact that quantitative statistics of QC cell number and division phenotypes are based on 2-dimensional (2D) imaging.

Here, we studied the QC region using 3D image analysis to deliver a quantitative description of the QC cell number, volume and division patterns in wild-type plants and QC division-activated lines. Furthermore, we demonstrate that *ERF115* and *CYCD1;1* not only promote periclinal (resulting in a new cell wall parallel to the root cap surface) but also anticlinal (resulting in a cell wall perpendicular to the nearest cell surface) QC cell divisions (Shishkova *et al.*, 2008), whereas cytokinin and ethylene rather appear to control the QC cell division plane.

Materials and Methods

Plant materials and growth conditions

All the genotypes used are in the Col-0 genetic background. The transgenic lines *ERF115^{OE}* and *ERF115^{SRDX}* were described previously (Heyman *et al.*, 2013). *pWOX5:ER-GFP* seeds were kindly provided by Prof. Ben Scheres (Xu *et al.*, 2006). The *pWOX5:CYCD1;1* construct was cloned by inserting the 3021-bp promoter region upstream of the *WOX5* start codon in front of the *CYCD1;1* coding sequence into the *pK7m24GW3* expression vector using Multisite Gateway® recombination. Transgenic *Arabidopsis thaliana* lines were subsequently generated through Agrobacterium-mediated transformation using the floral dip method (Clough and Bent, 1998). Single-locus lines were retained, and homozygous lines were selected using 40 mg/L kanamycin.

Plants were grown under a 16-h/8-h light/dark photoperiod and 70 $\mu\text{mol}\cdot\text{s}^{-1}\cdot\text{m}^{-2}$ of light strength on agar-solidified culture medium (2.15 g/L Murashige and Skoog (MS) medium, 10 g/L sucrose, 0.5 g/L 2-(*N*-morpholino) ethanesulfonic acid (MES), and 1% plant tissue culture agar, adjusted to pH 5.7) at 21°C after imbibition at 4°C in the dark for two days.

Hormone treatment

Seeds harboring the *pWOX5:ER-GFP* construct were sown on ½ MS medium supplemented with

either 100 nM 6-benzylaminopurine (BA) in dimethyl sulfoxide (DMSO) or 50 μ M 1-amino-1-cyclopropane carboxylic acid (ACC) in 10% ethanol, then grown for five days under a 16-h/8-h light/dark cycle at 21°C. For the control, respectively DMSO or ethanol was added to the medium.

Cell wall staining

We used a modified protocol based on Kurihara *et al.* (2015) in order to stain the cell walls. Transgenic *pWOX5:ER-GFP* seedlings were fixed with 4% paraformaldehyde (PFA) in 1 x PBS for 1 h at room temperature. Then, the seedlings were washed twice with 1x PBS and transferred to ClearSee solution (xylitol (10%, w/v), sodium deoxycholate (15%, w/v) and urea (25%, w/v) in H₂O) overnight. Thereafter, we stained the cell walls by imbibing the plants for 1 h in 0.1% Calcofluor White in ClearSee solution, washing them with ClearSee solution once and finally keeping the samples in the ClearSee solution before mounting them on microscope slides.

EdU labelling

In order to perform EdU labelling, 4-day-old seedlings were first transferred to $\frac{1}{2}$ MS medium supplemented with 10 μ M EdU (Invitrogen™ Click-iT™ EdU Cell Proliferation Kit for Imaging, Alexa Fluor™ 488 dye) for 24h, then the samples were fixed with 4% PFA in 1x PME (0.05 M piperazine-*N,N'*-bis(2-ethanesulfonic acid) (PIPES), 5mM MgSO₄ and 1mM ethylene glycol-bis(β -aminoethyl ether)-*N,N,N',N'*-tetraacetic acid (EGTA), adjusted to pH 6.9) overnight. After discarding the PFA, the seedlings were washed twice with 1x PME. Next, the root tips were dissected and placed in a drop of 1x PME on a SUPERFROST (adhesive) microscope slide. Once all samples were ready, the PME was removed and the root tips let drying at room temperature overnight. The day after, the root tips were washed with 1x PBS for 15 min. Following this step, the cell walls were degraded by incubating the samples with enzyme solution (1% cellulose, 0.5% cytohelicase and 1% pectolyase in 1x PME) for 1h at 37°C. We then washed the samples four times with 1x PBS (5 min for each time), with an additional wash with 1x PBS + 3% bovine serum albumin (BSA). Later, the roots tips were incubated in a permeabilization solution (3% IGEPAL, 10%DMSO in 1x PME) for 1h at room temperature and thereafter again washed twice with 1x PBS and two supplemental times with 1x PBS + 3% BSA. Subsequently, Click-It solution was added (40 μ l 10x Click-iT reaction buffer, 400 μ l distilled water, 10 μ l Copper protectant, 1 μ l Alexa Flour picolyl azide and 50 μ l Reaction buffer additive, all reagents come from the same kit as EdU) and the samples were consequently left in the dark at room temperature for 30 min. A subsequent wash with 1x PBS + 3% BSA performed before adding 100 μ l of Hoechst (in a 1/500 dilution) from the kit per slide, which were incubated in the dark at room temperature for 30 min (8 min vacuum and 22 min atmospheric pressure). Finally, wash twice with 1x PBS before mounting.

Confocal microscopy

Images of the QC zone in *pWOX5:ER-GFP* seedlings were taken using a Zeiss LSM 710 confocal microscope with a 40x water objective and pinhole was kept at 1 airy unit. For high-resolution z-stack scans, we set the interval of every two images between 0.1 to 0.12 μm . The Calcofluor White signal was detected after excitation with a 405nm laser within the 410–461 nm emission spectrum. The GFP was excited using a 488-nm laser and the emitted signal was captured within the 493–598 nm range. The two signals were acquired in a sequential order by using independent tracks. For EdU-DAPI staining, z-stacks were recorded over a 30 μm range at 0.5 μm step size using a Leica SP8X Confocal microscope and 40x water objective. EdU was excited using 488 nm Laser and emission was captured at 510-550 nm. DAPI was excited using 405 nm UV laser and emission was captured at 430-460 nm. Pinhole was kept at 1.7 airy units. Snapshot of cross section images of QC cells were obtained using the orthogonal sectioning mode of LAS X Viewer.

Cell segmentation and volume measurement

The 3D data was extracted from z-stack scanning pictures and analyzed by the MorphoGraphX software (<http://www.MorphoGraphX.org>). First, we used the pixel edit to remove extra tissues and cells around the QC cells under the work stack. Second, Gaussian blur was applied with a sigma of $0.4 \times 0.4 \times 0.2 \mu\text{m}^3$ using the process "Stack/Filters/Gaussian Blur Stack". Third, the cells were segmented using the auto-seed watershed segmentation process ("Stack/ITK/ITK Watershed Auto Seeded") with a level of 450. In addition, the obtained mesh was manual reviewed to ensure the accuracy of the automatic segmentation. Finally, we manually deleted the non-QC cells before extracting the 3D meshes of the remaining QC cells. The later step was performed using the process "Mesh/Creation/Marching Cubes 3D", by setting both cube size and smooth parameters to "1". The output was a 3D heat map in which cells were colored according to their volume within a 0-300 μm^3 range (process "Mesh/Heat Map/Heat Map"). The detailed position and volume information of each cell was finally exported for later QC cell average volume and QC zone total volume analysis.

Results

Three-dimensional imaging of the quiescent zone reveals up to eleven QC cells

On basis of longitudinal microscopic sections (along XY-axes) the QC is schematized as four-to-eight cells that are partitioned between two layers in the Z-axis. However, 2D cross-sections have limited power to observe and define cell numbers and division patterns. To gain a more accurate insight into the cell number and morphology, it is necessary to obtain a 3D level description and quantification of the QC zone. To be able to visualize specifically the QC cells, we used seedlings harboring the QC-specific marker *pWOX5:ER-GFP*. In order to obtain clear cell outlines and GFP signal, we performed Calcofluor White cell wall staining and ClearSee

for increased transparency (Kurihara *et al.*, 2015). Thereafter, the seedlings were mounted on a microscope slide and a general electrical tape was placed between the slide and the cover glass as a support to avoid deformation of the root cylinder, which could affect the volumetric measurements. High-resolution z-stack scanning pictures of root tips were taken by confocal laser scanning microscopy. After reconstructing the GFP-positive cells using MorphoGraphX software, the volumetric data of the full 3D QC zone were extracted and analyzed (Barbier de Reuille *et al.*, 2015). The output was converted to a 3D heat map in which cells were colored according to their volume (from blue to red, for small to large volumes, respectively). Using this pipeline, we identified on average 9.64 ± 1.44 cells being *pWOX5:ER-GFP*-positive within five-day-old Col-0 root tips (Table 1). Among these cells, 8.76 ± 1.09 were arranged in a flat round monolayered disk with an estimated diameter of $23.35 \pm 1.35 \mu\text{m}$ (Fig. 1A). The average volume of a QC cell was $191.70 \pm 16.02 \mu\text{m}^3$, while the volume of the QC zone was $1675.51 \pm 227.35 \mu\text{m}^3$. To facilitate visualization of the number of cells and their respective fluorescence intensities at different longitudinal sections, we numbered the QC cells in the transversal section (Fig. 1A). The longitudinal sections showed the classical view of up to four adjacent *pWOX5:ER-GFP*-positive cells (Fig. 1B-G). In 12 out of 25 seedlings analyzed, some GFP signal could be detected outside of the disk in the cortex and endodermis initials or their daughter cells (Table 1 and Supplementary Fig. S1). In these cells, the GFP signal intensity was weaker than that observed in the cells composing the QC zone, which might indicate residual *WOX5* promoter activity or carry-over of GFP inherited from the mother cell. Those cells only accounted for 9.13% of the cells expressing *pWOX5:ER-GFP*.

The organization and number of QC cells was confirmed by EdU staining (Fig. 1H), showing that following a 24h EdU labelling period 5-day-old Col-0 seedlings typically held an Edu positive ring of likely initial cells, encircling a disk of EdU negative ones (Fig. 1H and Table 2). Typically, 0-to-2 of the encircled cells positioned on the edge of the disk stained EdU positive, likely representing QC cells that underwent a round of DNA replication within this 24h time period. Exceptionally (1 out of 12 plants analyzed) showed three EdU positive nuclei in the disk zone, likely due to a recent cell division event as illustrated by the pairwise appearance of two of the labelled nuclei (Supplementary Fig. S2). This low number of EdU positive cells fits with the occurrence of only infrequent cell divisions within the assigned QC population. On average 5-day-old wild-type seedlings held 8.75 ± 0.62 QC cells of which 1 ± 1.04 cells (11.43%) were engaged in cell division (Table 2), confirming the 3D analysis.

Quantification of the change of QC cell number and volume over time

It has been reported that the QC cell proliferation rate increases with seedling age, correlated

with a decrease in QC cell size (Baum *et al.*, 2002; Timilsina *et al.*, 2019). To quantitatively decipher the QC growth dynamics, we imaged the QC zones of three-, five-, seven- and ten-day-old seedlings. By doing so, we were able to evaluate changes in QC cell number as well as changes in total QC region and single QC cell volume to ultimately infer the cell division patterns (Fig. 2A, B). The total number of QC cells increased from 6.61 ± 0.98 in three-day-old seedlings to 8.76 ± 1.09 in five-day-old seedlings, then reached 9.85 ± 1.23 in seven-day-old seedlings and finally 11.50 ± 1.79 in ten-day-old seedlings (Fig. 2E). During this time span, we found that the frequency of QC periclinal division was 0%, 1.39%, 4.79% and 11.76% in 3, 5, 7 and 10-day-old seedlings (Figure 2C). Thus, periclinal divisions occurred only rarely between three to ten days, as previously reported (Rahni and Birnbaum, 2019), but increased over time. From five to seven days, 12.44% (increase from 8.76 to 9.85) of QC cells underwent anticlinal or periclinal division, which is roughly the same as the 11.43% EdU positive QC cells observed in the EdU labeling experiment. Nevertheless, the average number of QC cells in a single layer (referred to as QC monolayer from here on) was 6.61 ± 0.98 in three-day-old seedlings, 8.64 ± 0.95 in five-day-old seedlings, 9.40 ± 1.05 in seven-day-old seedlings and 10.20 ± 0.89 in ten-day-old seedlings (Fig. 2D).

Correlated with an increase in the QC cell number, there was a significant drop of the average QC cell volume from $240.27 \pm 31.83 \mu\text{m}^3$ (SD) at day three to $191.70 \pm 16.02 \mu\text{m}^3$ (SD) at day five, and it continuously decreased to $169.36 \pm 27.81 \mu\text{m}^3$ (SD) at day seven and $167.98 \pm 17.63 \mu\text{m}^3$ (SD) at day ten (Fig. 2G). In contrast, the total QC volume increased from $1568.38 \pm 169.91 \mu\text{m}^3$ (SD) at day three to $1918.54 \pm 267.64 \mu\text{m}^3$ (SD) at day ten (Fig. 2H). Surprisingly, the average diameter of the QC zone fluctuated in only a narrow range, i.e. between 23.42 and 24.11 μm in three- and ten-day-old seedlings, respectively (Fig. 2F), although the total number of QC cells continuously increased (Fig. 2E) and the total volume of the QC zone slightly enlarged (Fig. 2H) when comparing ten- with three-day-old seedlings.

Analysis of QC parameters in QC division-activated genotypes

Previous studies have demonstrated that overexpression of *ERF115* and ectopic expression of *CYCD1;1* driven by the *WOX5* promotor resulted in disturbed QC cell division patterns (Forzani *et al.*, 2014; Heyman *et al.*, 2013). Conversely, no change in QC cell number was reported for plants expressing a dominant-negative *ERF115^{SRDX}* allele (Heyman *et al.*, 2013). To quantitatively map the described changes, we quantified the number of QC cells in the *ERF115^{OE}*, *ERF115^{SRDX}* and *pWOX5:CYCD1;1* transgenic lines.

Phenotypically, the *ERF115^{OE}*, *ERF115^{SRDX}* and *pWOX5:CYCD1;1* seedlings displayed a

slightly shorter root length compared to Col-0 (Supplementary Fig. S3A, C), but the axial cell arrangement and layers remained unchanged (Supplementary Fig. S3B). The length of the meristematic zone in *ERF115^{SRDX}* seedlings was larger (Supplementary Fig. S3D) and the cortex meristematic cell number of *pWOX5:CYCD1;1* was decreased compared to wild-type plants (Supplementary Fig. S3E), but overall, no major changes in root meristem structure could be observed for the different genotypes.

Subsequently, for each genotype the QC zone was determined (Fig. 3A-H and Supplementary Movies S1-4). The total QC cell numbers of *ERF115^{OE}* (13.60 ± 1.90), *ERF115^{SRDX}* (9.75 ± 1.21) and *pWOX5:CYCD1;1* (23.70 ± 2.25) were significantly increased compared with Col-0 (8.65 ± 1.35 ; Fig. 3K). Periclinal QC cell divisions could be observed in the median longitudinal sections of all five-day-old *ERF115^{OE}* and *pWOX5:CYCD1;1* seedlings (Fig. 3B, D), as previously described (Forzani *et al.*, 2014; Heyman *et al.*, 2013), but only in six out of 20 Col-0 seedlings and in five out of 20 *ERF115^{SRDX}* plants (Fig. 3A, C). The number of QC cells dividing periclinally accounted for 32.18% and 86.25% of the QC cell number in *ERF115^{OE}* and *pWOX5:CYCD1;1* seedlings, respectively (Fig. 3I), resulting in a bilayer of QC cells (Supplementary Movies S2 and S4). In contrast, in Col-0 and *ERF115^{SRDX}* seedlings this was only 4.88% and 3.72% (Fig. 3I). Further analysis showed that the number of QC cells in a single layer of *ERF115^{OE}* (10.10 ± 1.07) and *pWOX5:CYCD1;1* (12.63 ± 0.96) significantly increased compared to Col-0 (8.2 ± 1.44 ; Fig. 3J). Surprisingly, a small but statistically significant increase of the QC cell number was observed as well in the *ERF115^{SRDX}* root (9.4 ± 1.19), suggesting some residual ERF115 activity (Fig. 3J). *ERF115^{OE}* and *pWOX5:CYCD1;1* seedlings harbored smaller QC cells compared with Col-0 ($195.04 \pm 32.99 \mu\text{m}^3$, $155.79 \pm 29.21 \mu\text{m}^3$ and $234.58 \pm 45.23 \mu\text{m}^3$, respectively; Fig. 3E, F and H) but had a bigger total QC zone (Fig. 3L).

ACC and BA treatments cause an increased frequency of periclinal QC divisions

A variety of plant hormones are reported to induce QC cell division. Here, we quantified the number of QC divisions promoted by excessive cytokinin or ethylene (Ortega-Martínez *et al.*, 2007; Zhang *et al.*, 2013) in five-day-old seedlings germinated on medium holding 100 nM BA or 50 μM ACC, respectively. For each treatment the QC zone was determined as described above (Fig. 4A-H). The total QC cell number of seedlings grown on 100 nM BA (10.14 ± 1.71) significantly increased than on DMSO control (8.64 ± 1.29) (Fig. 4K). Compared to the DMSO control, the periclinal division frequency of QC cells increased sharply from 2.70% to 45.77% following BA treatment (Fig. 4I). In contrast, the QC cell monolayer cell number was significantly reduced from 8.41 ± 1.05 to 6.76 ± 1.30 (Fig. 4J). In addition, the average QC cell

volume increased from $189.25 \pm 24.45 \mu\text{m}^3$ to $236.02 \pm 59.16 \mu\text{m}^3$, and the total QC zone volume increased from $1632.46 \pm 330.60 \mu\text{m}^3$ to $2367.17 \pm 628.37 \mu\text{m}^3$ (Fig. 4L, M).

Like the BA treatment, ACC caused 22.75% of the QC cells to divide periclinally, compared to 1.08% in the ethanol control, but did only result in a statistically significant change in the QC monolayer cell number, not the total QC number (Fig. 4N-P). However, it resulted in an increase from $183.62 \pm 16.54 \mu\text{m}^3$ to $211.16 \pm 25.02 \mu\text{m}^3$ in average QC cell volume and from $1618.94 \pm 231.33 \mu\text{m}^3$ to $1970.61 \pm 394.81 \mu\text{m}^3$ in total QC zone volume (Fig. 4Q, R).

Discussion

WOX5:ER-GFP-positive cells are predominantly located in a monolayered disk zone

Using a 3D imaging pipeline, we demonstrated the number of QC cells within the stem cell niche to be close to eight. In longitudinal root sections of five-day-old seedlings, typically two to four QC cells could easily be recognized based on their location, morphological properties and use of QC-specific markers. In addition, upon propidium iodide staining, the outline of this small group of cells is more pronounced compared to the neighboring cells. As propidium iodide staining binds pectin, the more intense staining likely reflects a thicker cell wall that might be linked to the lower cell division rate. This thickened cell wall represents a straightforward manner to identify QC cells even without the help of a marker, such as *pWOX5:ER-GFP*. However, only the two cells in the middle of the four cells are commonly considered as QC cells, with the other peripheral cells being annotated as CEI cells. Nevertheless, we found these peripheral QC cells to show frequently a *WOX5:ER-GFP* signal as intense as that of the central cells, indicative that they are true QC rather than CEI cells. With 25 seedlings analyzed, 90.87% of the GFP-positive cells were found to be arranged in a flat monolayered disk, coinciding with the QC cells with a thicker boundary observed in the longitudinal sections. The remaining 9.13% of GFP-positive cells that were located outside of this disk likely represent true CEI cells and their daughters. The weaker GFP signal observed in these CEI cells might be explained by the signal stability of the carry-over of ER-GFP or by CEI cells retaining some partial QC identity. However, it has been demonstrated before through laser ablation experiments and clonal analysis that the position rather than the lineage determines cell fate (Kidner *et al.*, 2000; van den Berg *et al.*, 1995; van den Berg *et al.*, 1997). Therefore, the 9.13% of cells were not counted here as QC cells, despite their *pWOX5:ER-GFP* signal. Reversely, even in cases that the GFP signal intensity of individual cells located in QC monolayered disk zone was significantly lower compared to adjacent cells, we still considered them as being a QC cell.

The QC cell population increases in young seedlings but the diameter of the QC zone remains stable

To analyze and quantify the division patterns of QC cells over age, we investigated the number of QC cells in three- to ten-day-old seedlings. The number of periclinally divided QC cells was zero for three-day-old and one in three five-day-old seedlings, whereas in total nine periclinally divided QC cells were found in eight seven-day-old seedlings. This is consistent with the results of a week-long root meristem cell divisions tracking experiment, where imaging of two-day-old seedlings for up to 168 h allowed to visualize only one dividing QC cell (Rahni and Birnbaum, 2019). However, as most reported QC cell division data has been obtained from 2D images, it neglects any potential anticlinal division that may increase the size of the QC population. Our 3D images allowed to take these divisions into account. The average cell number within the QC monolayer rose from 6.61 ± 0.98 in three-day-old seedlings to 8.64 ± 0.95 in five-day-old seedlings, an increase of 30.71% in two days. The subsequent anticlinal division rate slowed down because there was no statistical difference between five- and seven-day-old seedlings, nor between seven- and ten-day-old ones. Nevertheless, the QC cell number reached 10.20 ± 0.89 in the ten-day-old seedlings, which was an increase of 54.31% compared to three-day-old seedlings, indicating that on average half of the QC cells had divided anticlinal during the seven-day span. It shows that QC cells divide more often anticlinal than periclinal, by which they might be less 'quiescent' as previously anticipated. However, due to the variability of the division rate and the lack of data after ten-day-old seedlings, it is difficult to accurately define the QC cell division rate.

Interestingly, from three- to ten-day-old seedlings, the average diameter of the QC zone fluctuated only slightly between 23.19 to 24.11 μm , being a difference of less than 1 μm . It means that even when half of the QC cells underwent anticlinal division, it did not affect the spatial position of QC population in the stem cell niche. Frequent anticlinal and occasional periclinal divisions only contributed to a 22.33% increase in total volume of the QC zone.

ERF115 and CYCD1;1 promote QC cell division in multiple dimensions

Both *ERF115^{OE}* and *pWOX5:CYCD1;1* transgenic lines have been reported to display an increased QC division rate (Forzani *et al.*, 2014; Heyman *et al.*, 2013). By applying 3D imaging, we could precisely map the effects of these transgenes on the frequency of periclinal and anticlinal QC divisions. For both lines, an increase in both division types could be observed, with the anticlinal divisions resulting in an increase in number of cells in the monolayer. Combined, these divisions resulted in a dramatic increase in total QC cell number, with the number being 1.5 times higher in *ERF115^{OE}* and almost tripled in *pWOX5:CYCD1;1*. Although

an effect on the total QC volume was observed as well, it was less outspoken because of a decrease in volume of the individual QC cells, likely due to the increased cell division rate. Overall, our data illustrate a multi-dimensional effect of both genes on QC division.

Surprisingly, the total QC cell number was not only increased in *ERF115^{OE}* but in the *ERF115^{SRDX}* line as well. The number of anticlinal cell divisions was increased in both genotypes, whereas the number of periclinal divisions only increased in the *ERF115^{OE}* line. This indicates that the *ERF115^{SRDX}* allele might retain some activity but not sufficiently high to drive periclinal divisions. Its lower potency to induce cell division compared to the wild-type allele explains its ability to operate as a dominant-negative allele under conditions that require a high level of ERF115 activity, such as following root tip excision or severe cell death owing to treatment with DNA damage-inducing agents (Heyman *et al.*, 2016; Heyman *et al.*, 2013), whereas its residual activity might still drive cell division upon ectopic activation in cells that lack wild-type ERF115 activity. However, we cannot rule out the possibility that ERF115 activity mainly determines the orientation of the cell division without changing overall mitotic activity, which is in accordance with the unaltered meristem size in the *ERF115^{SRDX}* line.

Periclinal divisions of the QC cells maintain a minimally sized QC population upon cytokinin and ethylene treatments

The exogenous application of many different plant hormones has been reported to trigger periclinal QC cell divisions, and hence are expected to result in an increase in QC cell number. For example, cytokinin induces the production of extra QC cells that maintain only partial QC identity (Zhang *et al.*, 2013). In contrast, newly generated QC cells resulting from ethylene treatment maintain expression of QC-specific marker genes (Ortega-Martínez *et al.*, 2007). Here, we confirmed the activation of periclinal QC divisions by the cytokinin BA and the ethylene precursor ACC, with the effect being most outspoken for the former. On the contrary, the number of QC cells in the monolayer was significantly reduced following cytokinin or ethylene treatment, suggesting that BA and ACC inhibit anticlinal cell divisions in favor of periclinal ones. In both cases the total QC volume increased because of an increased volume of the individual cells. The lack of an increase in total QC number following ethylene treatment indicates that this hormone specifically acts on the orientation of QC cell division, rather than cell division rate, whereas cytokinin controls both the QC division plane orientation and division rate.

In summary, 3D imaging in combination with cellular analysis using MorphoGraphX allowed us to accurately observe the number, volume and division pattern of QC cells in wild-type, transgenic and hormone-treated seedlings, revealing the effects on both the periclinal and

anticlinal QC divisions by hormones and transgenes. Our MorphoGraphX-based analysis pipeline revealed an average QC cell number of 6.61 in three-day-old seedlings, with a steady increase in cell number over the following days, whereas the diameter and overall volume of the QC region remained mostly unaltered. Therefore, although the QC zone in general remains rather static over time, the organization of the cells that occupy it may be slightly more dynamic than originally accepted. This dynamic trend, however, is still much more static compared to the surrounding stem cells.

Supplementary data

Supplementary Fig. S1. *pWOX5:ER-GFP* activity in CEI cells.

Supplementary Fig. S2. Cross section of a five-day-old Col-0 seedling counterstained with DAPI and S-phase label EdU.

Supplementary Fig. S3. Root phenotyping of five-day-old seedlings.

Supplementary Movie S1. QC zone of a 5-day-old Col-0 seedlings, as shown in Figure 4E.

Supplementary Movie S2. QC zone of a 5-day-old *ERF115^{OE}* seedlings, as shown in Figure 4F.

Supplementary Movie S3. QC zone of a 5-day-old *ERF115^{SRDX}* seedlings, as shown in Figure 4G.

Supplementary Movie S4. QC zone of a 5-day-old *pWOX5: CYCD1;1* seedlings, as shown in Figure 4H.

Data availability statement

The data supporting the findings of this study are available from the corresponding author, (Lieven De Veylder), upon request.

Acknowledgments

The authors thank Annick Bleys for help in preparing the manuscript. This work was supported by grants from the Research Foundation Flanders (G007218N and G010820N). R.L. was supported by the China Scholarship Council (201704910848).

Author contributions

RL conducted all experiments, performed formal analysis, curated all data, wrote the original draft and was involved in the final editing. BC, AB and JH provided materials and guidance and were involved in final editing. LDV conceived and supervised the project, wrote the original draft of the paper and was involved in final editing. All authors read and approved the final manuscript.

References

- Aida M, Beis D, Heidstra R, Willemsen V, Blilou I, Galinha C, Nussaume L, Noh Y-S, Amasino R, Scheres B.** 2004. The *PLETHORA* genes mediate patterning of the *Arabidopsis* root stem cell niche. *Cell* **119**, 109-120.
- Barbier de Reuille P, Routier-Kierzkowska A-L, Kierzkowski D, Bassel GW, Schüpbach T, Tauriello G, Bajpai N, Strauss S, Weber A, Kiss A, Burian A, Hofhuis H, Sapala A, Lipowczan M, Heimlicher MB, Robinson S, Bayer EM, Basler K, Koumoutsakos P, Roeder AHK, Aegerter-Wilmsen T, Nakayama N, Tsiantis M, Hay A, Kwiatkowska D, Xenarios I, Kuhlemeier C, Smith RS.** 2015. MorphoGraphX: A platform for quantifying morphogenesis in 4D. *eLife* **4**, e05864.
- Baum SF, Dubrovsky JG, Rost TL.** 2002. Apical organization and maturation of the cortex and vascular cylinder in *Arabidopsis thaliana* (Brassicaceae) roots. *American Journal of Botany* **89**, 908–920.
- Canher B, Heyman J, Savina M, Devendran A, Eekhout T, Vercauteren I, Prinsen E, Matosevich R, Xu J, Mironova V, De Veylder L.** 2020. Rocks in the auxin stream: wound-induced auxin accumulation and *ERF115* expression synergistically drive stem cell regeneration. *Proceedings of the National Academy of Sciences of the United States of America* **117**, 16667-16677.
- Chen Q, Sun J, Zhai Q, Zhou W, Qi L, Xu L, Wang B, Chen R, Jiang H, Qi J, Li X, Palme K, Li C.** 2011. The basic helix-loop-helix transcription factor MYC2 directly represses *PLETHORA* expression during jasmonate-mediated modulation of the root stem cell niche in *Arabidopsis*. *Plant Cell* **23**, 3335-3352.
- Clough SJ, Bent AF.** 1998. Floral dip: a simplified method for *Agrobacterium*-mediated transformation of *Arabidopsis thaliana*. *Plant Journal* **16**, 735-743.
- Clowes FAL.** 1954. The promeristem and the minimal constructional centre in grass root apices. *New Phytologist* **53**, 108–116.
- Cruz-Ramírez A, Díaz-Triviño S, Wachsman G, Du Y, Arteága-Vázquez M, Zhang H, Benjamins R, Blilou I, Neef AB, Chandler V, Scheres B.** 2013. A SCARECROW-RETINOBLASTOMA protein network controls protective quiescence in the *Arabidopsis* root stem cell organizer. *PLoS Biology* **11**, e1001724.
- Dolan L, Janmaat K, Willemsen V, Linstead P, Poethig S, Roberts K, Scheres B.** 1993. Cellular organisation of the *Arabidopsis thaliana* root. *Development* **119**, 71-84.
- Drisch RC, Stahl Y.** 2015. Function and regulation of transcription factors involved in root apical meristem and stem cell maintenance. *Frontiers in Plant Science* **6**, 505.
- Efroni I, Mello A, Nawy T, Ip P-L, Rahni R, DelRose N, Powers A, Satija R, Birnbaum KD.** 2016. Root regeneration triggers an embryo-like sequence guided by hormonal interactions. *Cell* **165**, 1721-1733.
- Forzani C, Aichinger E, Sornay E, Willemsen V, Laux T, Dewitte W, Murray JAH.** 2014. *WOX5* suppresses *CYCLIN D* activity to establish quiescence at the center of the root stem cell niche. *Current Biology* **24**, 1939-1944.
- Fujie M, Kuroiwa H, Kawano S, Kuroiwa T.** 1993. Studies on the behavior of organelles and

- their nucleoids in the root apical meristem of *Arabidopsis thaliana* (L.) Col. *Planta* **189**, 443-452.
- González-García MP, Vilarrasa-Blasi J, Zhiponova M, Divol F, Mora-García S, Russinova E, Caño-Delgado AI.** 2011. Brassinosteroids control meristem size by promoting cell cycle progression in *Arabidopsis* roots. *Development* **138**, 849-859.
- Grieneisen VA, Xu J, Marée AFM, Hogeweg P, Scheres B.** 2007. Auxin transport is sufficient to generate a maximum and gradient guiding root growth. *Nature* **449**, 1008-1013.
- Haecker A, Groß-Hardt R, Geiges B, Sarkar A, Breuninger H, Herrmann M, Laux T.** 2004. Expression dynamics of *WOX* genes mark cell fate decisions during early embryonic patterning in *Arabidopsis thaliana*. *Development* **131**, 657-668.
- Heyman J, Cools T, Canher B, Shavialenka S, Traas J, Vercauteren I, Van den Daele H, Persiau G, De Jaeger G, Sugimoto K, De Veylder L.** 2016. The heterodimeric transcription factor complex ERF115-PAT1 grants regeneration competence. *Nature Plants* **2**, 16165.
- Heyman J, Cools T, Vandenbussche F, Heyndrickx KS, Van Leene J, Vercauteren I, Vanderauwera S, Vandepoele K, De Jaeger G, Van Der Straeten D, De Veylder L.** 2013. ERF115 controls root quiescent center cell division and stem cell replenishment. *Science* **342**, 860-863.
- Hoermayer L, Montesinos JC, Marhava P, Benkova E, Yoshida S, Friml J.** 2020. Wounding-induced changes in cellular pressure and localized auxin signalling spatially coordinate restorative divisions in roots. *Proceedings of the National Academy of Sciences of the United States of America* **117**, 15322-15331.
- Kidner C, Sundaresan V, Roberts K, Dolan L.** 2000. Clonal analysis of the *Arabidopsis* root confirms that position, not lineage, determines cell fate. *Planta* **211**, 191-199.
- Kurihara D, Mizuta Y, Sato Y, Higashiyama T.** 2015. ClearSee: a rapid optical clearing reagent for whole-plant fluorescence imaging. *Development* **142**, 4168-4179.
- Lozano-Elena F, Planas-Riverola A, Vilarrasa-Blasi J, Schwab R, Caño-Delgado AI.** 2018. Paracrine brassinosteroid signaling at the stem cell niche controls cellular regeneration. *Journal of Cell. Science* **131**, jcs204065.
- Matosevich R, Cohen I, Gil-Yarom N, Modrego A, Friedlander-Shani L, Verna C, Scarpella E, Efroni I.** 2020. Local auxin biosynthesis is required for root regeneration after wounding. *Nature Plants* **6**, 1020-1030.
- Nawy T, Lee J-Y, Colinas J, Wang JY, Thongrod SC, Malamy JE, Birnbaum K, Benfey PN.** 2005. Transcriptional profile of the *Arabidopsis* root quiescent center. *Plant Cell* **17**, 1908-1925.
- Ortega-Martínez O, Pernas M, Carol RJ, Dolan L.** 2007. Ethylene modulates stem cell division in the *Arabidopsis thaliana* root. *Science* **317**, 507-510.
- Pi L, Aichinger E, van der Graaff E, Llavata-Peris CI, Weijers D, Hennig L, Groot E, Laux T.** 2015. Organizer-derived *WOX5* signal maintains root columella stem cells through chromatin-mediated repression of *CDF4* expression. *Developmental Cell* **33**, 576-588.
- Rahni R, Birnbaum KD.** 2019. Week-long imaging of cell divisions in the *Arabidopsis* root meristem. *Plant Methods* **15**, 30.
- Rovere FD, Fattorini L, Ronzan M, Falasca G, Altamura MM.** 2016. The quiescent center and the stem cell niche in the adventitious roots of *Arabidopsis thaliana*. *Plant Signaling & Behavior* **11**, e1176660.
- Sabatini S, Heidstra R, Wildwater M, Scheres B.** 2003. SCARECROW is involved in positioning the stem cell niche in the *Arabidopsis* root meristem. *Genes & Development* **17**, 354-358.
- Sarkar AK, Luijten M, Miyashima S, Lenhard M, Hashimoto T, Nakajima K, Scheres B, Heidstra R, Laux T.** 2007. Conserved factors regulate signalling in *Arabidopsis thaliana* shoot and root stem cell organizers. *Nature* **446**, 811-814.
- Sena G, Wang X, Liu H-Y, Hofhuis H, Birnbaum KD.** 2009. Organ regeneration does not require a functional stem cell niche in plants. *Nature* **457**, 1150-1153.
- Shishkova S, Rost TL, Dubrovsky JG.** 2008. Determinate root growth and meristem maintenance in Angiosperms. *Annals of Botany* **101**, 319-340.

- Timilsina R, Kim JH, Nam HG, Woo HR.** 2019. Temporal changes in cell division rate and genotoxic stress tolerance in quiescent center cells of *Arabidopsis* primary root apical meristem. *Scientific Reports* **9**, 3599.
- Ugaratechea-Chirino Y, Swarup R, Swarup K, Péret B, Whitworth M, Bennett M, Bougourd S.** 2010. The AUX1 LAX family of auxin influx carriers is required for the establishment of embryonic root cell organization in *Arabidopsis thaliana*. *Annals of Botany* **105**, 277–289.
- van den Berg C, Willemsen V, Hage W, Weisbeek P, Scheres B.** 1995. Cell fate in the *Arabidopsis* root meristem determined by directional signalling. *Nature* **378**, 62-65.
- van den Berg C, Willemsen V, Hendriks G, Weisbeek P, Scheres B.** 1997. Short-range control of cell differentiation in the *Arabidopsis* root meristem. *Nature* **390**, 287-289.
- Vilarrasa-Blasi J, González-García MP, Frigola D, Fàbregas N, Alexiou KG, López-Bigas N, Rivas S, Jauneau A, Lohmann JU, Benfey PN, Ibañes M, Caño-Delgado AI.** 2014. Regulation of plant stem cell quiescence by a brassinosteroid signaling module. *Developmental Cell* **30**, 36-47.
- Xu J, Hofhuis H, Heidstra R, Sauer M, Friml J, Scheres B.** 2006. A molecular framework for plant regeneration. *Science* **311**, 385-388.
- Zhang H, Han W, De Smet I, Talboys P, Loya R, Hassan A, Rong H, Jürgens G, Knox JP, Wang M-H.** 2010. ABA promotes quiescence of the quiescent centre and suppresses stem cell differentiation in the *Arabidopsis* primary root meristem. *Plant Journal* **64**, 764-774.
- Zhang W, Swarup R, Bennett M, Schaller GE, Kieber JJ.** 2013. Cytokinin induces cell division in the quiescent center of the *Arabidopsis* root apical meristem. *Current Biology* **23**, 1979-1989.
- Zhou W, Lozano-Torres JL, Blilou I, Zhang X, Zhai Q, Smant G, Li C, Scheres B.** 2019. A jasmonate signaling network activates root stem cells and promotes regeneration. *Cell* **177**, 942-956.

Table 1. QC cell quantification in *pWOX5:ER-GFP* five-day-old seedlings^a

Line #	1	2	3	4	5	6	7	8	9	10	11	12	13	14	15	16	17	18	19	20	21	22	23	24	25	Average (\pm SD)
Number of GFP-positive cells (\pm SD)	12	9	8	8	8	9	10	9	9	12	10	10	10	10	7	10	11	9	12	11	7	11	9	9	11	9.64 \pm 1.44
Number of GFP-positive cells in QC zone (\pm SD)	10	9	8	8	8	7	10	9	8	10	10	9	8	10	7	9	8	9	10	11	7	9	9	8	8	8.76 \pm 1.09

^aData resulting from three independent biological repeats

Table 2. Quantification EdU positive cells in QC region in Col-0 5-day-old seedlings ^a													
Line #	1	2	3	4	5	6	7	8	9	10	11	12	Average (\pm SD)
Number of QC cells (\pm SD)	8	8	10	9	9	9	9	9	8	9	8	9	8.75 \pm 0.62
Number of EdU positive cells located in QC zone (\pm SD)	0	0	1	0	2	0	1	3	2	1	2	0	1.00 \pm 1.04

^aData resulting from three independent biological repeats

FIGURES

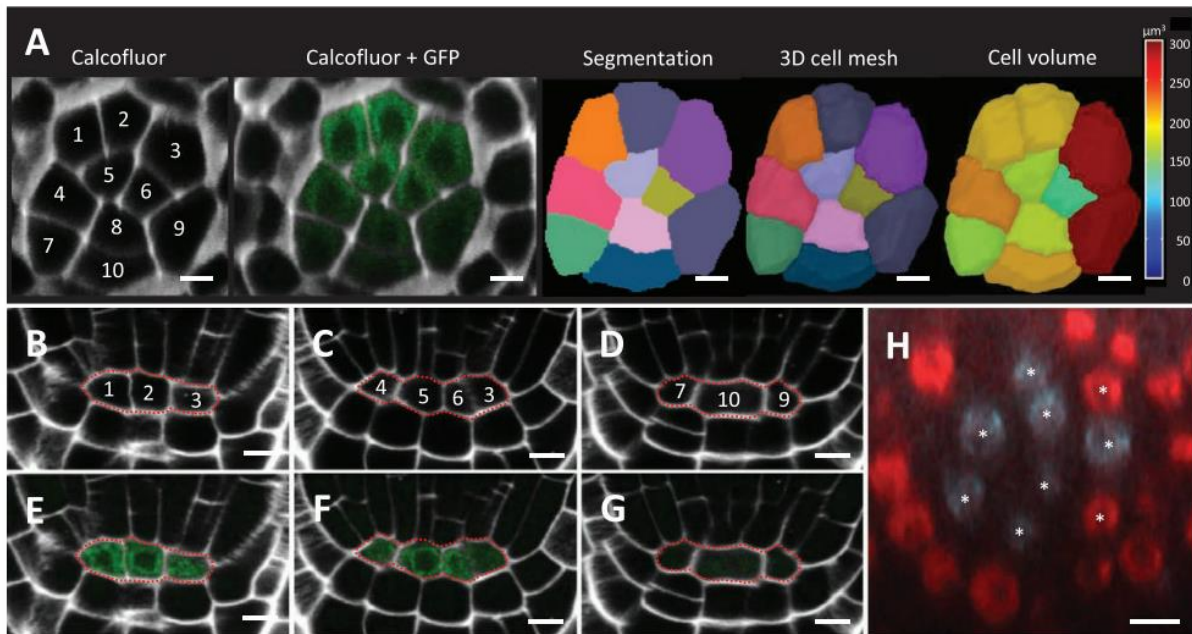


Fig. 1. Schematic representation of the steps used to delineate the QC zone. (A) Visual representation of the different steps in the pipeline for generating a 3D digital QC cell zone, including capturing of raw data and MorphoGraphX-based auto seeded watershed segmentation, extraction of 3D cell meshes with marching cubes and generation of a cellular volume heat map (0-300 μm^3 range). (B-G) Longitudinal section through the obtained 3D image of a five-day-old *pWOX5:ER-GFP* seedling counterstained with Calcofluor White, either numbered (according to the image in (A)) (B-D) or showing GFP fluorescence (E-G). The fluorescence intensity of QC cells in Fig. 1G was weaker than in Figures 1E-F due to the distance from the laser, photobleaching and phototoxicity after the long-time imaging required for obtaining the required imaging details needed for the MorphoGraphX pipeline, but they were still positive compared to neighboring negative cells. (H) Representative cross section of a five-day-old Col-0 seedling counterstained with DAPI and S-phase label EdU. DAPI is shown in cyan and EdU is shown in red. The QC zone is outlined by the red dashed line in B-G and QC cells are marked with white asterisks in H. Scale bars = 5 μm .

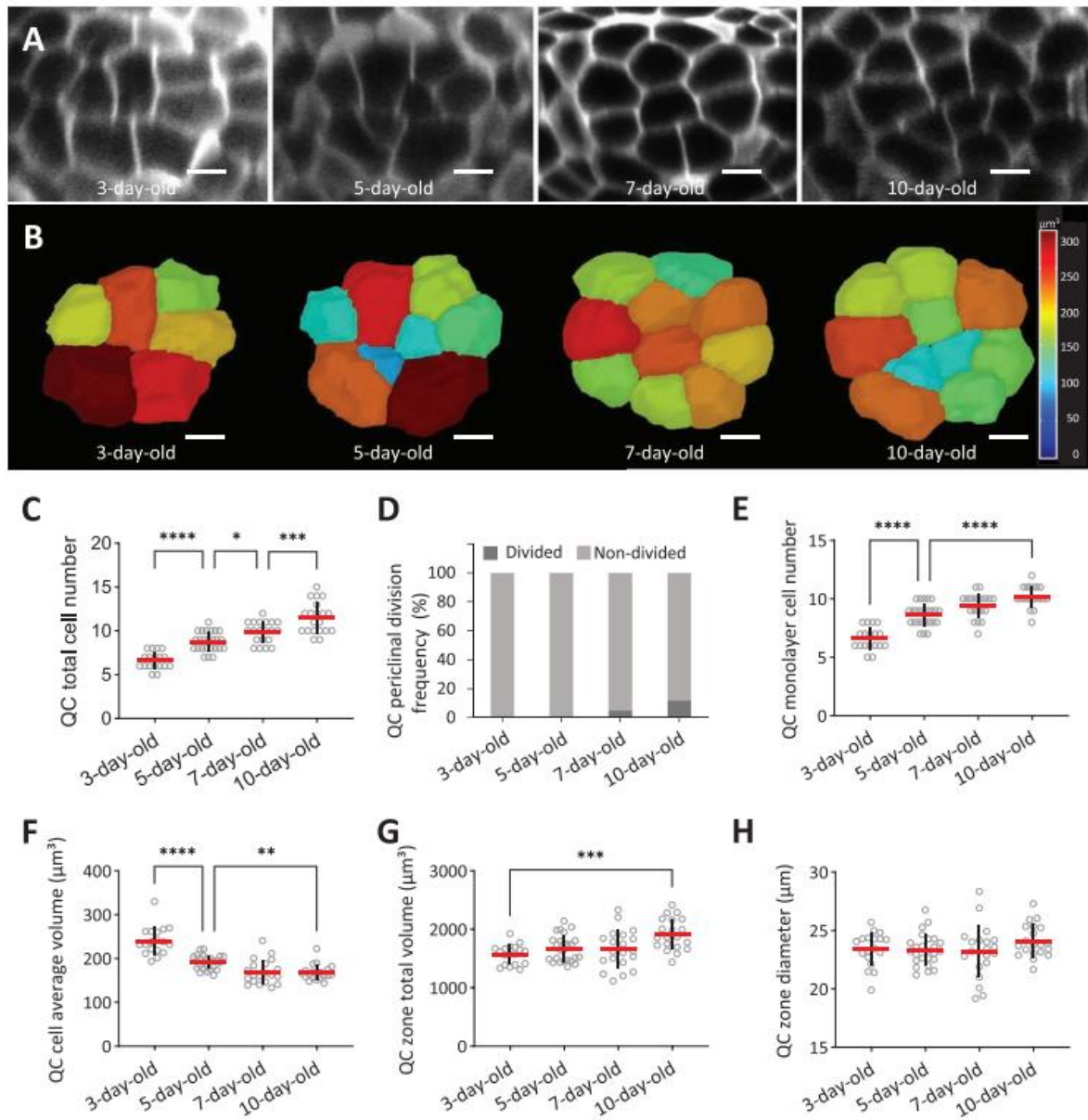


Fig. 2. QC cellular changes in young seedlings. (A) Cross sections of three- to ten-day-old *pWOX5:ER-GFP* seedlings counterstained with Calcofluor White. (B) Heat map of QC cell volumes in three- to ten-day-old *pWOX5:ER-GFP* seedlings (0-300 μm^3 range). (C-H) Frequency of periclinal QC divisions (C), cell number within the QC monolayer (D), total number of QC cells (E), diameter of the QC zone (F), average volume of the QC cells (G) and total volume of the QC zone of three-, five-, seven- and ten-day-old seedlings (H). Scale bars are 5 μm . Data are from three independent biological repeats (with total number of roots quantified being 18, 25, 20 and 20 for three-, five-, seven- and ten-day-old seedlings, respectively, and minimum number per biological repeat being five). All individual data points are plotted. Red horizontal lines represent the mean and black vertical lines represent error bars \pm SD. Asterisks indicate significance levels by one-way ANOVA and Tukey's multiple comparison tests (* $p < 0.05$, ** $p < 0.01$, *** $p < 0.001$, **** $p < 0.0001$).

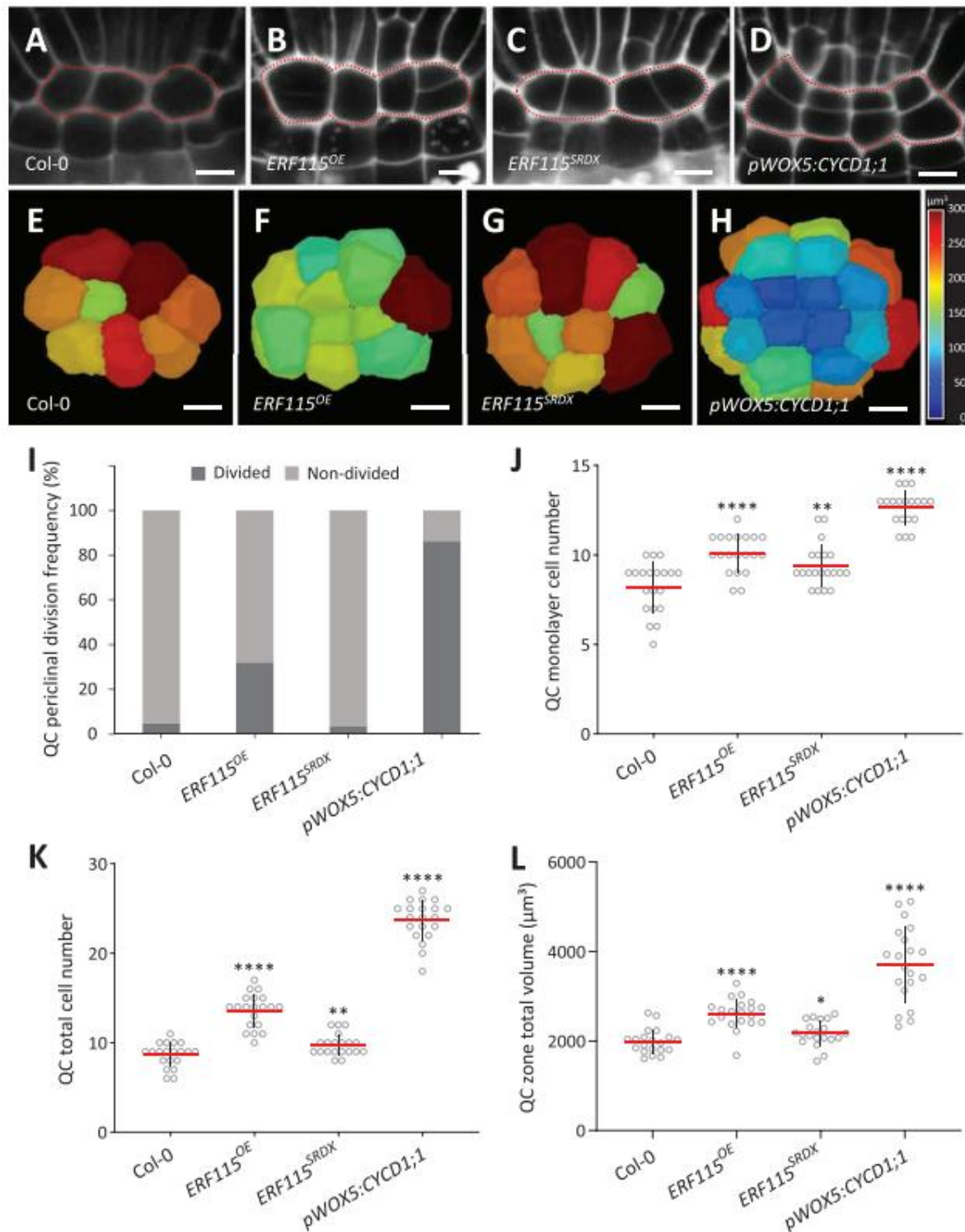


Fig. 3. QC quantification in five-day-old seedlings. (A-D) Longitudinal sections of Col-0, *ERF115^{OE}*, *ERF115^{SRDX}* and *pWOX5:CYCD1;1* seedlings counterstained with modified pseudo-Schiff propidium iodide. The QC zones are outlined by red dashed lines. (E-H) Heat map of the QC cell volumes of Col-0, *ERF115^{OE}*, *ERF115^{SRDX}* and *pWOX5:CYCD1;1* seedlings (0-300 μm³ range). Scale bars = 5 μm. (I-L) Quantification of the frequency of periclinal QC divisions (I), cell number within the QC monolayers (J), total number of QC cells (K), and total

volume of QC zone (L) in Col-0, *ERF115^{OE}*, *ERF115^{SRDX}* and *pWOX5:CYCD1;1* seedlings. Data are from three independently biological repeats (with total number of roots quantified being 20 for each genotype and minimum number per biological repeat being five). All individual data points are plotted. Red horizontal lines represent the mean and black vertical lines represent error bars \pm SD. Asterisks indicate significance levels by ANOVA single factor (*p < 0.05, **p < 0.01, ***p < 0.0001).

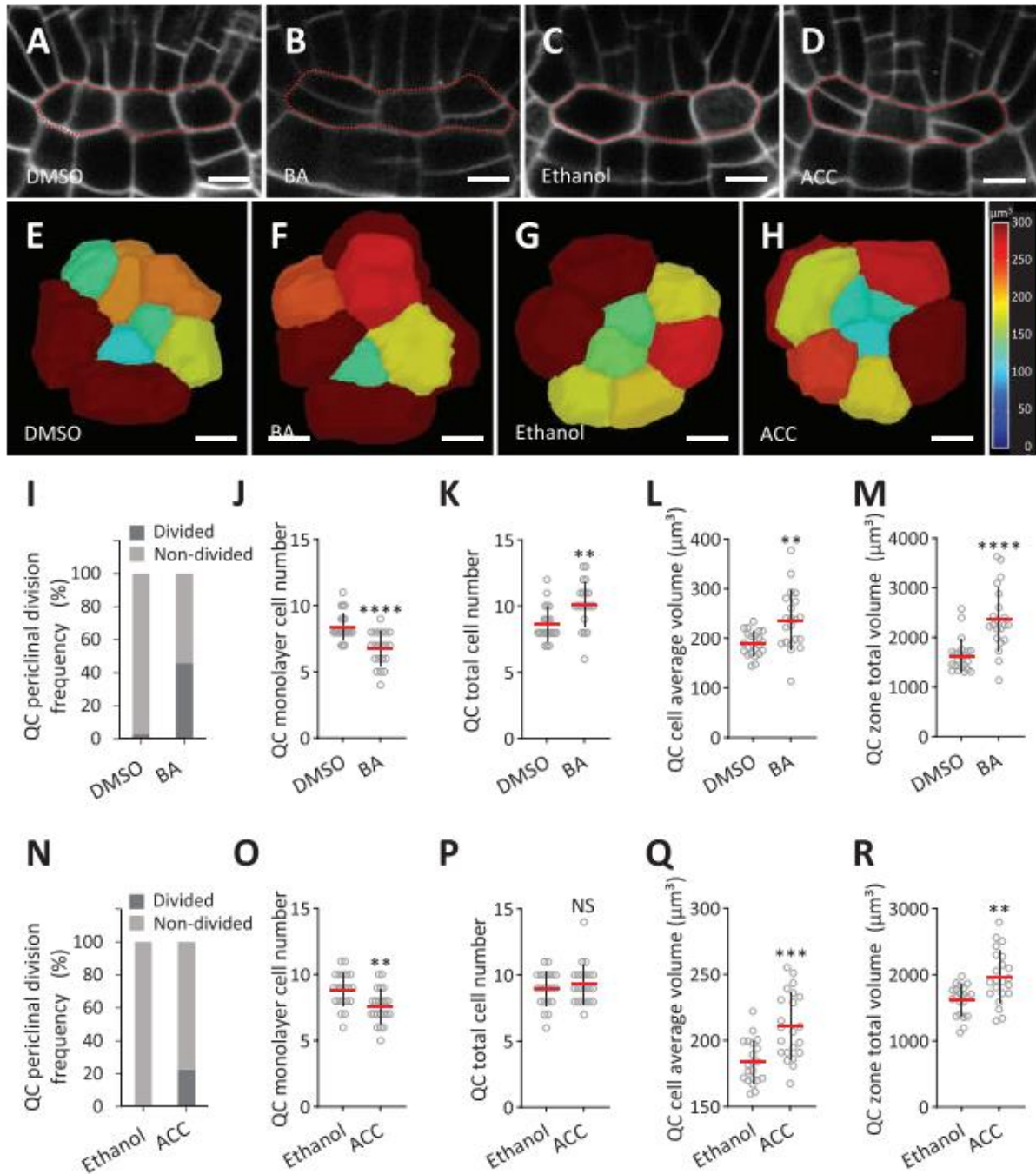


Fig. 4. QC characterization following treatment of 5-day-old seedlings with BA or ACC. (A-D) Longitudinal sections of *pWOX5:ER-GFP* seedlings treated with DMSO (A), 100 nM BA (B), ethanol (C) or 50 μM ACC (D), counterstained with Calcofluor White. The QC zones are outlined by red dashed lines. (E-H) Heat map of the QC cell volumes of *pWOX5:ER-GFP* seedlings treated with DMSO (E), BA (F), ethanol (G) and ACC (H) (0-300 μm³ range). Scale bars = 5 μm. (I-M) Quantification of the frequency of periclinal QC divisions (I), cell number within the QC monolayers (J), total number of QC cells (K), average volume of QC cells (L), and total volume of QC zone (M) in *pWOX5:ER-GFP* seedlings treated with DMSO or 100 nM BA. (N-R) Quantification of the frequency of periclinal QC divisions (N), cell number within the

QC monolayers (O), total number of QC cells (P), average volume of QC cells (Q), and total volume of QC zone (R) in *pWOX5:ER-GFP* seedlings treated with ethanol or 50 μ M ACC. Data are from three independently biological repeats (with total number of roots quantified being 22, 21, 21, 22 for DMSO, BA, Ethanol and ACC respectively, and minimum number per biological repeat being five). All individual data points are plotted. Red horizontal lines represent the mean and black vertical lines represent error bars \pm SD. Asterisks indicate significance levels by ANOVA single factor (NS means not significant, **p < 0.01, ***p < 0.001, ****p < 0.0001).